Quadrupole coupling and crystal-field shielding in $CaF_2:Eu^{3+}:O^{2-}$ under hydrostatic pressure

Andrzej P. Radliński and A. J. Silversmith*
Department of Solid State Physics, Research School of Physical Sciences, The Australian National University, GPO Box 4, Canberra, A.C.T. 2601 Australia
(Received 25 November 1985)

The nuclear quadrupole interactions in the $^7F_0$ ground electronic state and the $^5D_0$ excited state of the $^{151}Eu^{3+}$ and $^{153}Eu^{3+}$ ions have been investigated by optical means. The optically detected nuclear quadrupole resonance, excitation, and luminescence of the Eu^{3+}-O^{2-} C_{3v} symmetry center have been studied at 4.2 K in single crystals of CaF_2:Eu:O under hydrostatic pressure up to 7.5 kbar. An energy-level diagram of the lower ^7F_J electronic states has been established. The two dominating components of the hyperfine quadrupole energy for ^{151}Eu have been determined: $P_{\rm lat}=-22$ MHz, $P^{(2)}_{4f}(^7F_0)=+29$ MHz. Their pressure derivatives are -20 ± 2 and $+16\pm2$ kHz/kbar, respectively. The value of the crystal-field parameter $A^0_2\langle r^2\rangle=615$ cm^{-1} has been found. From the experimentally determined sum of the electronic shielding factors $(R_Q+\sigma_2)\cong0$ it has been concluded that shielding of the crystal field at the $4f^6$ electronic shell is very small. The pressure derivatives of the electronic shielding factors have been estimated for the first time: $\partial[(1-\gamma_\infty)+80(R_Q+\sigma_2)]/\partial p=(5\pm1)\times10^{-2}$ kbar^{-1}.

I. INTRODUCTION

A theory of hyperfine interactions in the $^7F_0$ ground state of trivalent europium was published by Elliott[1] in 1957. Both the hyperfine magnetic and quadrupole interactions were considered up to second order. The most remarkable prediction regarded substantial quenching of the nuclear magnetic moment by the interactions with the low-lying $^7F_1$ multiplet. This fact makes conventional NMR experiments difficult and there are indeed very few NMR experimental data reported on Eu^{3+} systems.[2] With the advent of high-resolution laser spectroscopy, both hole-burning and optically detected nuclear-magnetic-resonance (ODNMR) techniques were used to study Eu^{3+} ions in various hosts.[3–7] These studies were mostly concentrated on the nuclear magnetic properties and general agreement with Elliott's original predictions was demonstrated. On the other hand, the origin of the quadrupolar interaction received relatively little attention.[6] In the present work we concentrate on this particular area.

Elliott[1] predicted that the main contribution to the electric field gradient interacting with the Eu^{3+} nuclear quadrupolar moment was due to the second-order effect of polarization of the $4f^6$ electrons, whereas the first-order lattice effect contributed a few percent of the total energy of interaction. The shielding and antishielding effects were not taken into account. This omission was first corrected by Judd *et al.*[8] Through the subsequent work of Edmonds[9] and Blok and Shirley[10] the subject of the quadrupolar interaction in the Eu^{3+} ion was presented with a broader background of various aspects of the shielding phenomena in the rare-earth-metal ions.[11–13] It turned out that the first-order lattice effects were of similar magnitude but of opposite sign to those of second order mentioned above, mainly due to the large negative antishielding factor γ_∞ characteristic of the rare-earth series. In order to enable a full description of the two electric field gradient components, information regarding both the nuclear (quadrupole) and electronic (crystal-field) splittings is necessary.

In this work we study a Eu^{3+} ion charge compensated by a nearby O^{2-} ion in the CaF_2 lattice. In our previous papers an account of both optical[14] and magnetic nuclear[7] properties of this C_{3v} symmetry center has been given. Here we present data regarding the effect of hydrostatic pressure on the optically detected nuclear quadrupole resonance (ODNQR) of the ^{151}Eu isotope in its ground $^7F_0$ and the excited $^5D_0$ electronic states, and of the ^{153}Eu isotope in its ground state in the pressure range of 1 to 7.5 kbar. Pressure dependence of some optical transitions within the $4f^6$ shell relevant to the interpretation of the ODNQR data is also reported. Magnitudes and pressure coefficients of the two dominating components of the electric field gradient are determined. These results are used to discuss the magnitude and pressure dependence of the electron shielding factors γ_∞, σ_2, and R_Q.

II. BACKGROUND

The Eu^{3+}-O^{2-} center studied here is of C_{3v} symmetry. Its quadrupolar nuclear and electronic z axes coincide with the crystallographic $\langle111\rangle$ directions.[7,14] This fact makes the analysis of the quadrupolar interactions relatively simple, reducing the generally tensorial calculations to the algebra of the diagonal z components of the electric field gradient. The effective axial quadrupolar Hamiltonian of a Eu nucleus in the absence of the external magnetic field has the form[1]

$$H=P(I_z^2-\tfrac{1}{3}I^2)\ . \tag{1}$$

For an axial center with the electronic and nuclear axes coinciding P can be written as[1,10]

$$P = P_{\text{lat}} + P_{4f}^{(2)} + P_{\text{ps}} , \tag{2}$$

where

$$P_{\text{lat}} = -\frac{3Q}{I(2I-1)}(1-\gamma_\infty)A_2^0 \tag{3}$$

and in the Russell-Saunders coupling scheme

$$P_{4f}^{(2)} = \frac{6e^2Q}{I(2I-1)} \frac{A_2^0\langle r^2\rangle(1-\sigma_2)}{\Delta_2}$$

$$\times\langle r^{-3}\rangle(1-R_Q)\,|\,\langle 2||\alpha||0\rangle\,|^2 , \tag{4}$$

where $\langle 2||\alpha||0\rangle = 0.224$ (0.059) for the $^7F_0$ ($^5D_0$) state, respectively. The difference between the former value and the previously published value of $2/5\sqrt{3}$ (for the $^7F_0$ state) is due the the admixture of ^5D states into the ground-state wave function. The values of $\langle 2||\alpha||0\rangle$ given above were calculated by standard methods using the Eu^{3+} free-ion wave functions given by Ofelt.[15] The quantity $P_{4f}^{(2)}(^5D_0)$ is small and therefore of secondary interest in the present analysis. To avoid lengthy labels we use the abbreviation $P_{4f}^{(2)} \equiv P_{4f}^{(2)}(^7F_0)$ throughout the rest of this paper. P_{ps} is a small pseudoquadrupolar contribution fully analyzed previously.[7] The meaning of symbols in Eqs. (1)—(4) is identical to those adopted by Blok and Shirley.[10]

III. EXPERIMENTAL

Polarization of emission lines in the spectral region 15 600—17 434 cm^{-1} (Ref. 14) was measured in a magnetic field of 5 T applied along the [111] crystal axis with monitoring of the emission in the direction perpendicular to the field. In this configuration only one subset of otherwise equivalent C_{3v} sites was excited by pumping selectively in the $^7F_0 \rightarrow {}^5D_2(E)$ transition region at 21 673 cm^{-1} and the σ and π components of the $^5D_0 \rightarrow {}^7F_J$ emission lines were monitored.

The pressure measurements were done with a Unipress beryllium-copper optical cell filled with petroleum spirit as a pressure-transmitting medium. At the temperature of 4.2 K the medium is solidified but the pressure remains hydrostatic.[16] A three-turn rf coil in which the sample was mounted was placed inside the cell. The cell itself was mounted in an optical cryostat in a gas-exchange chamber. The pressure was measured by monitoring the shift of the R_2 emission line in ruby.[17]

For the ODNQR measurements an unoriented single crystal of CaF_2:Eu^{3+}:O^{2-} was illuminated in resonance with the $^7F_0 \rightarrow {}^5D_0$ transition at 17 434 cm^{-1} with a single-mode, actively frequency-stabilized laser beam, and the strong $^5D_0 \rightarrow {}^7F_2(E)$ emission at 16 215 cm^{-1} was monitored with a lock-in detection system. For the precise determination of the ODNQR line shape the radio frequency was swept over regions of about 1 MHz in 1 min.

The pressure dependence of the $^7F_0 \rightarrow {}^5D_J$ and $^5D_0 \rightarrow {}^7F_J$ optical transitions was determined by excitation and luminescence measurements, respectively. Either the above-mentioned single-mode cw laser or a pulsed dye laser was used as an excitation source. The pressure shifts of the optical transitions were rather small compared to their linewidths and therefore only one or two highest-pressure experimental points was used to determine the values of the pressure coefficients. The majority of the spectra was taken at 4.2 K, but some measurements were also done at room temperature.

IV. RESULTS AND DISCUSSION OF THE OPTICAL SPECTROSCOPIC DATA

A. Energy-level diagram of the lowest ^7F_J states

Polarization measurements were undertaken to complement the previously published Zeeman data[14] in order to establish the energy level scheme for the lowest ^7F_J multiplets. Positions of some of these levels determine the size and character of the quadrupolar interactions. In particular, the crystal-field splitting of the $^7F_1$ multiplet is pro-

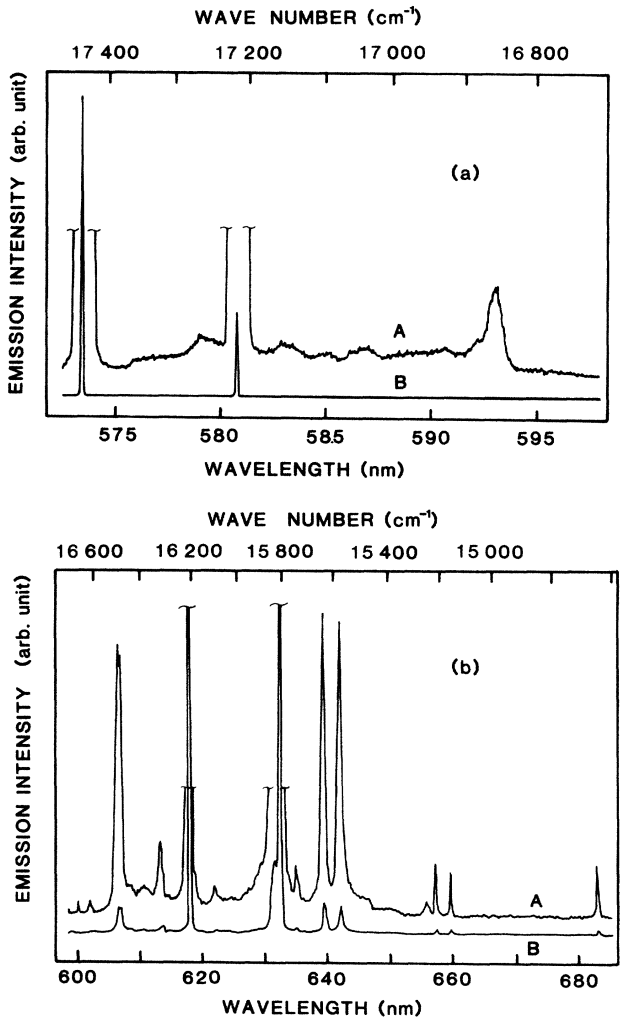

FIG. 1. Luminescence spectrum of the CaF_2:Eu:O system in the region of (a) the $^5D_0 \rightarrow {}^7F_0$, $^7F_1$ transitions, and (b) the $^5D_0 \rightarrow {}^7F_2$ transitions. The spectrum was obtained by exciting the $^7F_0 \rightarrow {}^5D_0$ transition at 17 434 cm^{-1}. Resolution in (a): A —4.0 Å, B —0.12 Å; resolution in (b): A —6 Å, B —0.6 Å.

TABLE I. Compilation of the Zeeman (Ref. 7) and polarization results for the $^5D_0 \rightarrow {}^7F_J$ emission. The electronic states of the ^7F_J multiplet are identified in the last column. Pol. denotes polarization.

Emission wave number (cm^{-1})	Distance from $^7F_0$ (cm^{-1})	g factor	Multipole term	Pol.	Interpretation of final state
17434	0	0	ED	π(7:1)	$^7F_0(A_1)$
17215	219	1.53	MD	π(3:1)	$^7F_1(E)$[a]
16854	~580			π(2:1)	
16697	737	3.0	ED	π(3:1)	$^7F_2(E)$[a,b]
16515	919			σ(1.7:1)	
16215	1219	$\lesssim$0.2	ED	π(5:1)	$^7F_2(A_1)$[a]
15845	1589			σ(1.3:1)	E[a]
15669	1765			π(2.5:1)	
15608	1826			π(2.5:1)	

[a]Symmetry label confirmed by magnetic circular emission (MCE).
[b]There is an apparent contradiction in the polarization dependence of this emission line.

portional to the crystal-field parameter A_2^0 which also determines the value of P_{lat} [Eq. (3)], whereas the $^7F_0$-$^7F_2(A_1)$ distance corresponds to the value Δ_2, which is present in expression (4) for $P_{4f}^{(2)}$. Positions of both $^7F_1(A_2)$ and $^7F_2(A_1)$ levels could not be determined from the Zeeman data only.

Figure 1 shows an overall luminescence spectrum in the region of the $^5D_0 \rightarrow {}^7F_1, {}^7F_2$ transitions taken at zero magnetic field. The spectrum was obtained by exciting the $^7F_0 \rightarrow {}^5D_0$ transition of 17434 cm^{-1} using a pulsed dye laser. Due to the experimental configuration employed during the polarization measurements the signal-to-noise ratio obtained there was approximately a factor of 10 lower than that shown in Fig. 1. Therefore it was not possible to obtain reliable polarization data for the weakest lines.

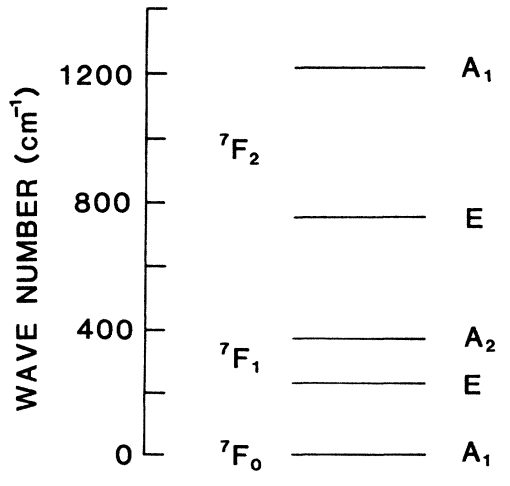

FIG. 2. Energy-level diagram of the lowest levels of the ^7F_J multiplet in CaF_2:Eu:O. Position of the $^7F_1(A_2)$ level shown here is only estimated. Position of one of the $^7F_2(E)$ levels could not be determined.

Comparison of Zeeman and polarization results is shown in Table I. Transitions listed there originate from an A_1 level. Selection rules in the C_{3v} symmetry are as follows: (1) electric dipole (ED) transitions to the A_1 levels are π polarized, to the E levels σ polarized; (2) magnetic dipole (MD) transitions to the A_2 levels are σ polarized, to the E levels are π polarized. Multipolarities of the optical transitions listed in Table I were predicted assuming pure Russell-Saunders coupling. The identifications presented in Table I remain in agreement with positions of $^7F_2(A_1)$ levels determined in many other Eu^{3+} systems.[18]

There is an apparent contradiction between the results for the 737 cm^{-1} level. Emission terminating at this level and originating from the $^5D_2(A_1)$ level is much stronger[14] than emission from the $^5D_0$ level and in fact this was used to determine the g value of this state. The g value is large and there is no doubt that the final state is $^7F_2(E)$. The polarization result may be explained by allowing for a MD component in the optical transition.

On the basis of the arguments presented above, the energy-level diagram of the lowest components of the ^7F_J term was constructed (Fig. 2). The approximate position of the $^7F_1(A_2)$ level was obtained from the ODNQR data as discussed in Sec. V C.

B. Shifts of the $4f^6$ levels under hydrostatic pressure

Relative pressure shifts of some of the ^7F_J levels are important for the analysis of the pressure ODNQR data. For completeness the pressure shifts of the ^5D_J levels were also investigated. Examples of experimental data for both the luminescence and excitation signals are shown in Fig. 3. The obtained results are compiled in Table II. As could be expected, the pressure shifts of the $4f^6$ states are rather small, of the order of several GHz/kbar. Since no distinct optical transition to the $^7F_1(A_2)$ state was observed the pressure dependence of this particular level could not be determined.

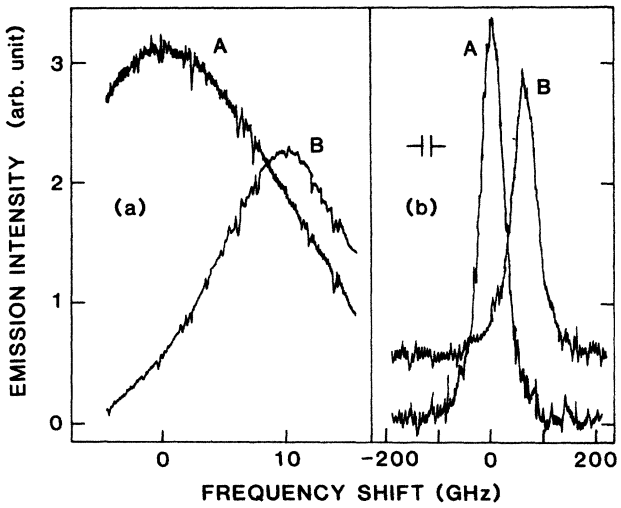

FIG. 3. Pressure shift of (a) the $^7F_0 \rightarrow {}^5D_0$ absorption line and (b) the $^5D_0 \rightarrow {}^7F_2(A_1)$ emission line in CaF_2:Eu:O at 4.2 K. $A-p=1$ bar, $B-p=6.6$ kbar. Spectral resolution is determined by the laser linewidth of ~ 2 MHz in (a), and the slit width in (b).

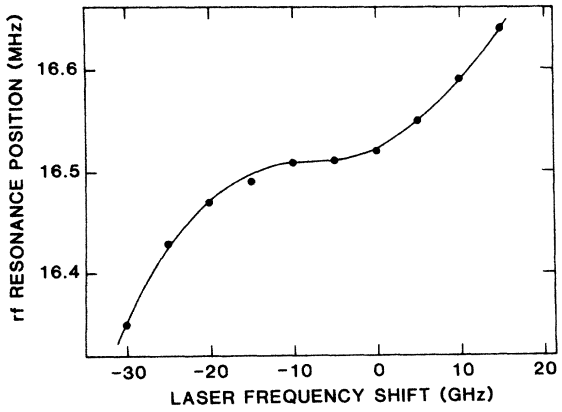

FIG. 4. Position of the ^{151}Eu $|\pm\frac{1}{2}\rangle \rightarrow |\pm\frac{3}{2}\rangle$ ground-state rf resonance at 16.52 MHz versus laser frequency shift with respect to the center of the $^7F_0 \rightarrow {}^5D_0$ absorption line at $p=1$ bar, $T=4.2$ K.

V. RESULTS AND DISCUSSION OF ODNQR DATA

A. Results

Both naturally abundant ^{151}Eu and ^{153}Eu isotopes have a nonzero nuclear spin ($I=\frac{5}{2}$) and therefore it is possible to employ the optical pumping cycle to saturate the nuclear-spin-allowed optical transitions between the hyperfine energy levels of the ground $^7F_0$ and excited $^5D_0$ states. The hyperfine structure is then probed by applying an rf field and monitoring the intensity of the emitted light. Positive ODNQR signals correspond to the ground-state hyperfine splittings, and negative signals to the excited state structure.[7] For an axial center one expects to observe two rf resonances associated with each electronic state ($^7F_0$ and $^5D_0$).

The inhomogeneous width [full width at half maximum (FWHM)] of the $^7F_0 \rightarrow {}^5D_0$ absorption line in CaF_2:Eu^{3+}:O^{2-} is 28 GHz at 4.2 K and positions of the rf resonances depend on the laser frequency within the line (Fig. 4). Therefore, in order to avoid systematic errors during the pressure experiments the laser frequency was kept tuned to the (pressure dependent) center of the line within the limits ± 1 GHz. Figure 5 shows a typical example of experimental data. The signal-to-noise ratio was critically dependent on the laser-frequency stability (jitter). The shifts of the rf resonances versus hydrostatic pressure are shown in Fig. 6. These data are summarized in Table III.

TABLE II. Shift of the optical transitions within the $4f^6$ shell in CaF_2:Eu:O under the hydrostatic pressure. lu denotes luminescence and ex denotes excitation.

Transition	Energy at 4.2 K (cm^{-1})	Mode of measurement	Pressure coefficient (GHz/kbar)
$^5D_0 \rightarrow {}^7F_1(E)$	17215	lu	$\lesssim 2.0(5)$[a]
$^5D_0 \rightarrow {}^7F_2(A_1)$	16215	lu	$+9.3(5)$[a]
$^7F_0 \rightarrow {}^5D_0(A_1)$	17434	ex[b]	$-1.5(2)$[a]
$^7F_0 \rightarrow {}^5D_1(E)$	19124	ex[c]	$-3.5(5)$[a]
			$-2.2(5)$[d]
$^7F_0 \rightarrow {}^5D_1(A_2)$	19262	ex[c]	$+1.0(5)$[d]
$^7F_0 \rightarrow {}^5D_2(E)$	21586	ex[c]	$-8.7(5)$[a]
$^7F_0 \rightarrow {}^5D_2(E)$	21673	ex[c]	$-3.8(5)$[a]
$^7F_0 \rightarrow {}^5D_2(A_1)$	21730	ex[c]	$-3.2(5)$[a]

[a]Measured at 4.2 K, $p \cong 7$ kbar.
[b]Measured with a cw single-mode laser.
[c]Measured with a pulsed dye laser.
[d]Measured at 300 K, $p \cong 13$ kbar.

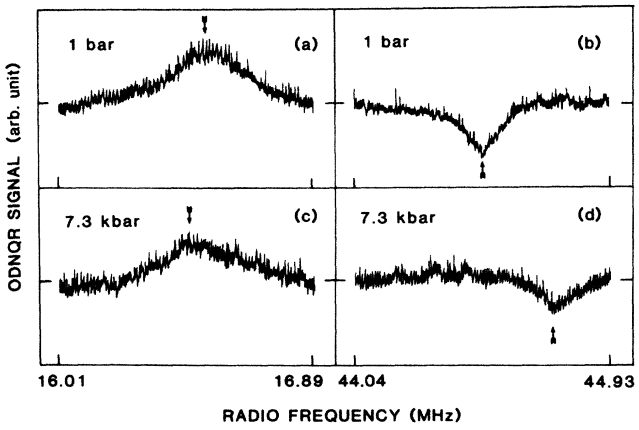

FIG. 5. ODNQR signals from the ^{151}Eu ground-state $|\pm\frac{1}{2}\rangle\rightarrow|\pm\frac{3}{2}\rangle$ rf transitions at (a) $p=1$ bar, (c) $p=7.3$ kbar, and from the ^{151}Eu excited state $|\pm\frac{1}{2}\rangle\rightarrow\pm\frac{3}{2}\rangle$ transitions at (b) $p=1$ bar and (d) $p=7.3$ kbar.

B. Electronic shielding factors: General remarks

Before analyzing our data we briefly recapitulate information available in the literature about the electronic shielding factors that enter the theory of quadrupolar hyperfine interactions through Eqs. (3) and (4).

The quadrupole antishielding factor γ_∞, which describes the enhancement of the electric field gradient at the nucleus due to the closed-shell distortion, appears to have a well-established value of $\gamma_\infty\cong-80$, approximately valid for the whole lanthanide series.[10,12,13] This value will be used throughout this work.

The atomic shielding factor R_Q for the case of the $4f$ electron is defined by a relation $\langle r^{-3}\rangle_{4f}=\langle r^{-3}\rangle_{at}(1-R_Q)$. No experimental values of R_Q are available for a Eu^{3+} ion and only the angular contribution $R_Q^{ang}(Eu^{3+})$ has been calculated.[19] However, this value is compatible with the later calculated angular components of R_Q for Pr^{3+} and Tm^{3+} (Ref. 13), which allows one to expect that $R_Q\approx0.13$ found there for these two ions should not be far away from the value for Eu^{3+}. Several experimentally determined values of R_Q are known: for the Tm^{3+} ion, Barnes *et al.*[20] find $R_Q=0.11$ in thulium ethyl sulfate, $R_Q=-0.01$ in Tm_2O_3, and deduce $R_Q=0.20$ from the data of Cohen[21] for Fe_2Tm. Hüfner *et al.*[22] obtain $R_Q\approx0.3$ for metallic erbium. Therefore, a range $0\lesssim R_Q\lesssim0.3$ may be expected for a Eu^{3+} on the basis of these experimental results. A variation of R_Q within similar limits may be calculated if one allows for small variations of some of the parameters of the theory.[13]

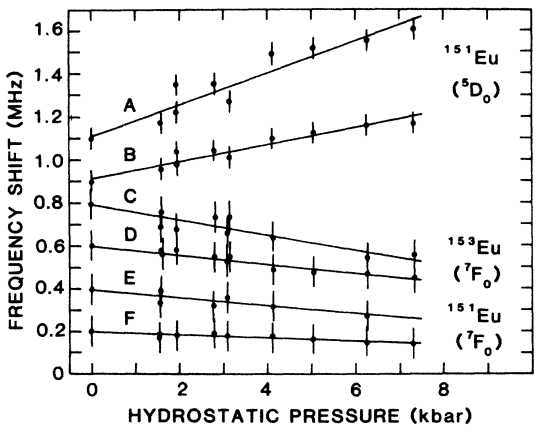

FIG. 6. Pressure shifts of the ODNQR lines with the hydrostatic pressure at $T=4.2$ K: ^{151}Eu excited state (A) $|\pm\frac{3}{2}\rangle\rightarrow|\pm\frac{5}{2}\rangle$ transition and (B) $|\pm\frac{1}{2}\rangle\rightarrow|\pm\frac{3}{2}\rangle$ transition; ^{153}Eu ground-state (C) $|\pm\frac{3}{2}\rangle\rightarrow|\pm\frac{5}{2}\rangle$ transition and (D) $|\pm\frac{1}{2}\rangle\rightarrow|\pm\frac{3}{2}\rangle$ transition; ^{151}Eu ground-state (E) $|\pm\frac{3}{2}\rangle\rightarrow|\pm\frac{5}{2}\rangle$ transition and (F) $|\pm\frac{1}{2}\rangle\rightarrow|\pm\frac{3}{2}\rangle$ transition. (Data are displaced for clarity.)

The shielding factor σ_2 is a measure of the closed-shell distortions experienced at the position of the $4f$ electrons. It is sensitive to the detailed density of the $4f$ electrons, and therefore depends intrinsically on the crystal-field potential (host dependence). Because of this complication its value is hard to calculate. The values of σ_2 obtained theoretically for the rare-earth ions are usually large ($\gtrsim0.5$),[23–26] except for the results of Burns[27] who predicts $\sigma_2\lesssim0.1$. Experimental results of $\sigma_2=0.73$ exist for the Eu^{3+} ion in europium ethyl sulfate.[10] Reference 10 lists experimentally determined values of σ_2 for all rare-earth ethyl sulfates, and all of them are large. However, there is a clear host-dependence effect, well illustrated in the case of thulium ethyl sulfate ($\sigma_2=0.71$) and Tm_2O_3 ($\sigma_2=0.41$).[20]

The analysis of the ODNQR results presented here is based on the data obtained for the ground $^7F_0$ and excited $^5D_0$ states of the ^{151}Eu isotope. Results for the ground state of the ^{153}Eu isotope are within experimental accuracy proportional to those of the ^{151}Eu isotope, the proportionality factor being the quadrupole moment ratio Q^{153}/Q^{151}.

C. Discussion of Results

1. *Ambient pressure results*

In these calculations, numerical results are given for ^{151}Eu; the values of P_{lat} and $P_{4f}^{(2)}$ for ^{153}Eu are larger by a factor equal to the quadrupole moment ratio of 2.54.[7]

Using the values of $\langle r^{-3}\rangle=49.19$ Å^{-3} (Ref. 10), $\langle r^2\rangle=0.233$ Å^2 (Ref. 6), and $Q^{151}=1.12\pm0.07$ b (Ref. 28) one can show that for the $^5D_0$ excited state the $P_{4f}^{(2)}$ contribution to the electric field gradient is about 3%. The pseudoquadrupolar contribution in this state is negligibly small, whereas it accounts for 0.70 MHz in the ground $^7F_0$ state.[7] Thus, using Eq. (3) and the experimental value of $P_{lat}(^5D_0)=-22.2$ MHz one calculates $A_2^0\langle r^2\rangle\cong615$ cm^{-1}. Substituting into Eq. (4) one calculates

$$P_{4f}^{(2)}\cong57.6(1-\sigma_2)(1-R_Q)\frac{A_2^0\langle r^2\rangle}{\Delta_2}\,, \tag{5}$$

where the result is expressed in MHz. Since the value of P_{lat} is independent of the electronic state, one can use

$\Delta_2 = 1219\ \text{cm}^{-1}$ (Table I) and $P(^7F_0) \cong +7.5$ MHz (Ref. 7) to obtain

$$(1-R_Q)(1-\sigma_2) \cong 1.02 \pm 0.02 \ . \tag{6}$$

This indicates that both R_Q and σ_2 are close to zero, in contrast to the few other characterized Eu^{3+} systems discussed in the previous section. There is apparently very little (if any) shielding of the interaction of the crystal field with the $4f^6$ shell in the CaF_2:Eu:O system, as indicated by the small value of σ_2.

On the basis of this result one can predict roughly the A_2-E crystal-field splitting Δ_1 of the $^7F_1$ level to be

$$\Delta_1 = \tfrac{3}{5}(1-\sigma_2)A_2^0\langle r^2\rangle \lesssim 370\ \text{cm}^{-1} \ . \tag{7}$$

This places the $^5D_0 \to {}^7F_1(A_2)$ luminescence line within the range of the phonon replicas of the $^5D_0 \to {}^7F_1(E)$ transition (Fig. 1). Such a degeneracy may explain why no sharp line corresponding to the $^5D_0 \to {}^7F_1(A_2)$ transition is observed. By the same token no distinct optical polarization effects should be expected.

2. *Hydrostatic pressure dependence*

From the experimental data for the $^5D_0$ and $^7F_0$ states (Table III) one obtains

$$\frac{\partial}{\partial p} P_{\text{lat}} = -(20 \pm 2)\ \text{kHz/kbar} \ , \tag{8a}$$

$$\frac{\partial}{\partial p} (P_{\text{lat}} + P_{4f}^{(2)}) = -(4 \pm 1)\ \text{kHz/kbar} \ , \tag{8b}$$

which yields

$$\frac{\partial}{\partial p} P_{4f}^{(2)} = (16 \pm 2)\ \text{kHz/kbar} \ . \tag{9}$$

On the basis of Eq. (4) this partial derivative can be expressed as

$$\frac{\partial}{\partial p} P_{4f}^{(2)} = P_{4f}^{(2)}(p=0) \left[\frac{\frac{\partial}{\partial p}(A_2^0\langle r^2\rangle)}{A_2^0\langle r^2\rangle} + \frac{\frac{\partial}{\partial p}[(1-R_Q)(1-\sigma_2)]}{(1-R_Q)(1-\sigma_2)} - \frac{1}{\Delta_2}\frac{\partial}{\partial p}\Delta_2 \right] . \tag{10}$$

The first term in the large parentheses can be calculated by differentiating (3):

$$\frac{\partial}{\partial p} P_{\text{lat}} = P_{\text{lat}}(p=0) \left[\frac{1}{1-\gamma_\infty}\frac{\partial}{\partial p}(1-\gamma_\infty) + \frac{1}{A_2^0\langle r^2\rangle}\frac{\partial}{\partial p}(A_2^0\langle r^2\rangle) \right] , \tag{11}$$

whereas the third term in (10) can be obtained from the spectroscopic data compiled in Table II. Because both R_Q and σ_2 are small compared to 1, Eq. (10) can be rewritten in the approximate form

$$\frac{\partial}{\partial p} P_{4f}^{(2)} \cong P_{4f}^{(2)}(p=0) \left[\frac{1}{P_{\text{lat}}^0}\frac{\partial}{\partial p}P_{\text{lat}} - \frac{1}{1-y_\infty}\frac{\partial}{\partial p}(1-\gamma_\infty) - \frac{\partial}{\partial p}(R_Q+\sigma_2) - \frac{1}{\Delta_2}\frac{\partial}{\partial p}\Delta_2 \right] , \tag{12}$$

where P_{lat}^0 stands for $P_{\text{lat}}(p=0)$. The first and the last terms contribute $+27 \pm 3$ and $+9 \pm 1$ kHz/kbar, respectively. The contribution due to the pressure dependence of the atomic shielding factors [the two middle terms in Eq. (12)] is -19 ± 4 kHz/kbar, well above the experimental error. Thus one gets

TABLE III. Positions and pressure derivatives of the rf resonances in the ODNQR spectrum of CaF_2:Eu:O measured at 4.2 K.

	$^7F_0$ ground-state resonances				$^5D_0$ excited state resonances	
Isotope	^{151}Eu		^{153}Eu		^{151}Eu	
Transition	$\lvert\pm\frac{1}{2}\rangle \to \lvert\pm\frac{3}{2}\rangle$	$\lvert\pm\frac{3}{2}\rangle \to \lvert\pm\frac{5}{2}\rangle$	$\lvert\pm\frac{1}{2}\rangle \to \lvert\pm\frac{3}{2}\rangle$	$\lvert\pm\frac{3}{2}\rangle \to \lvert\pm\frac{5}{2}\rangle$	$\lvert\pm\frac{1}{2}\rangle \to \lvert\pm\frac{3}{2}\rangle$	$\lvert\pm\frac{3}{2}\rangle \to \lvert\pm\frac{5}{2}\rangle$
Resonance Position (MHz)	16.52±0.02	33.08	39.85	79.76	44.46	88.97
Pressure coefficient (kHz/kbar)	−8±1	−20±2	−22±2	−39±2	+40±4	+75±4

$$\frac{\partial}{\partial p}[(1-\gamma_\infty)+80(R_Q+\sigma_2)] \cong +(5\pm 1)\times 10^{-2}\ \text{kbar}^{-1}\ , \tag{13}$$

where $1-\gamma_\infty=80$ was used. To the best of our knowledge this is the first experimental demonstration of the pressure dependence of electronic shielding factors in a crystal. No theoretical calculations of this effect are available either. It should be noted that the positive sign of the effect observed here indicates that the term 80 $\partial/\partial p(R_Q+\sigma_2)$ dominates over the pressure derivative of $1-\gamma_\infty$. One expects $\partial/\partial p(1-\gamma_\infty)$ to be negative, since under the influence of the external stress the F^- and O^{2-} ligands enter the peripherical regions of the Eu^{3+} ion $5p$ electronic outer shell [polarization of which is responsible for the large value of $1-\gamma_\infty$ (Ref. 13)], causing decrease of both the polarization and $1-\gamma_\infty$. Since σ_2 is known to depend most strongly on the host lattice, it is likely that its pressure derivative dominates over the other contributions in expression (13).

VI. CONCLUSION

The modified Elliott model of the hyperfine interactions in a Eu^{3+} center has been tested. The optical and ODNQR experimental data obtained from the CaF_2:Eu:O system under hydrostatic pressure were also analyzed. The magnitudes and pressure derivatives of the two components of the hyperfine quadrupole interaction, P_{lat} and $P_{4f}^{(2)}$, have been determined. It has been shown that the electronic shielding factors σ_2 and R_Q are both small. The electronic shielding factors have been demonstrated to be pressure dependent.

This work demonstrates the usefulness of optical techniques in studying subtleties of hyperfine nuclear interactions in lanthanide nuclei. Because the ODNQR is a resonant technique and enables access to excited electronic states, it provides more specific information than that available from either the nuclear alignment or the Mössbauer spectroscopic data. It is particularly useful in studies on Eu^{3+} centers where the NMR experiments are difficult to perform. Together with our previous work on the nuclear magnetic properties[7] this paper provides a detailed account of the hyperfine interactions in the CaF_2:$Eu^{3+}O^{2-}$ system.

ACKNOWLEDGMENTS

We would like to thank Dr. N. B. Manson for his involvement in the polarization and magnetic circular emission experiments and for helpful discussions.

*Present address: IBM Research Center, 850 Harry Road, K67/802, San Jose, CA 95120-6099

[1]R. J. Elliott, Proc. R. Soc. London Ser. B **70**, 119 (1957).
[2]R. L. Streever and P. J. Caplan, Phys. Rev. B **3**, 2910 (1971).
[3]L. E. Erickson and K. K. Sharma, Phys. Rev. B **24**, 3697 (1981).
[4]R. R. Shelby and R. M. Macfarlane, Phys. Rev. Lett. **47**, 1172 (1981).
[5]A. J. Silversmith and N. B. Manson, J. Phys. C **17**, L97 (1984); R. L. Cone, R. T. Harley, and M. J. M. Leask, *ibid.* **17**, 3101 (1984).
[6]K. K. Sharma and L. E. Erickson, J. Phys. C **18**, 2935 (1985).
[7]A. J. Silversmith, A. P. Radliński, and N. B. Manson, J. Phys. (Paris) Colloq. **46**, C7-531 (1985).
[8]B. R. Judd, C. A. Lovejoy, and D. A. Shirley, Phys. Rev. **128**, 1733 (1962).
[9]D. T. Edmonds, Phys. Rev. Lett. **10**, 129 (1963).
[10]J. Blok and D. A. Shirley, Phys. Rev. **143**, 278 (1966).
[11]R. Sternheimer, Phys. Rev. **84**, 244 (1951).
[12]R. E. Watson and A. J. Freeman, Phys. Rev. **135**, A1209 (1964).
[13]R. M. Sternheimer, Phys. Rev. **146**, 140 (1966).
[14]A. J. Silversmith and A. P. Radliński, J. Phys. C **18**, 4385 (1985).
[15]G. S. Ofelt, J. Chem. Phys. **38**, 2171 (1963).
[16]S. Wasilewski, A. M. Davidson, R. A. Stradling, and S. Porowski, *Application of High Magnetic Fields in Semiconductor Physics*, Vol. 177 of *Lecture Notes in Physics*, edited by G. Landwehr (Springer-Verlag, Berlin, 1983), p. 233; B. Gil, M. Baj, J. Camassel, H. Mathieu, C. Benoit à la Guillaume, N. Mestres, and J. Pascaul, Phys. Rev. B **29**, 3398 (1984).
[17]G. J. Piermarini, S. Block, J. D. Barnett, and R. A. Forman. J. Appl. Phys. **46**, 2774 (1975).
[18]E. V. Sayre and S. Freed, J. Chem. Phys. **24**, 1213 (1956); K. H. Hellwege, V. Hohnsen, H. G. Kahle, and G. Schaack, Z. Phys. **148**, 112 (1957); M. Faucher and P. Caro, J. Chem. Phys. **63**, 446 (1975); P. Porcher and P. Caro *ibid.* **65**, 89 (1976); J. Hölsa and P. Porcher, *ibid.* **75**, 2108 (1981); J. B. Gruber, R. P. Leavitt, C. A. Morrison, and N. C. Chang, *ibid.* **82**, 537 (1985).
[19]R. M. Sternheimer, Phys. Rev. **80**, 102 (1950).
[20]R. G. Barnes, R. L. Mössbauer, E. Kankeleit, and J. M. Poindexter, Phys. Rev. **136**, A175 (1964).
[21]R. L. Cohen, Phys. Rev. **134**, A94 (1964).
[22]S. Hüfner, P. Kienle, W. Wiedemann, and E. Eicher, Z. Phys. **182**, 499 (1985).
[23]C. L. Lenander and E. Y. Wong, J. Chem. Phys. **38**, 2750 (1963).
[24]R. E. Watson and A. J. Freeman, Phys. Rev. **133**, A1571 (1964).
[25]D. K. Ray, Proc. Phys. Soc. London **82**, 47 (1963).
[26]R. M. Sternheimer, M. Blume, and R. F. Peierls, Phys. Rev. **173**, 376, (1968).
[27]G. Burns, Phys. Rev. **128**, 2121 (1962).
[28]G. Guthohrlein, Z. Phys. **214**, 332 (1968).